Aprovechando las redes ZigBee y el enrutamiento avanzado para la recopilación y transferencia inmediata de datos UV

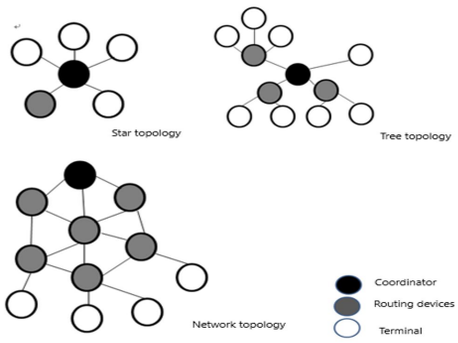

Harnessing ZigBee Networks and Advanced Routing for Immediate UV Data Collection and Transfer

Hua Ni [1], Jinting Xu [1], Zhangfeng Ruan [1], Qiang Li [2]

1 Institute of Metrology Inspection, Shanghai Institute of Quality Inspection and Technical Research, 900 Jiangyue Rd, Shanghai 201114, China
2 Consumer Lighting (Shanghai)Co.,Ltd.Testing Lab, China

The demand for real-time, efficient Ultraviolet (UV) monitoring has intensified to safeguard public health and environmental stability. Therefore, this article proposes a remote real-time monitoring transmission system for ultraviolet data through combining ZigBee and GPRS technology. UV data is captured using UVM-30A sensors, transmitted through a ZigBee network (via the CC2530 module) to a coordinator, and then sent to a host computer using a SIM800 GPRS module for continuous monitoring. The main findings include: An ant colony particle swarm optimization (ACO+PSO) algorithm enhances data transmission in large-scale networks. In mesh topologies with over 100 nodes, ACO+PSO ensures low transmission delays under high loads. For smaller networks, AODVjr proves more cost-effective. ZigBee's short-range transmission demands careful distance management to maintain data integrity. In addition to being within an effective distance range, it is also necessary to ensure a suitable packet transmission time interval. Experimental results reveal that longer intervals between data packets lower packet loss rates, while shorter intervals increase losses. The ZigBee + GPRS integration enables effective real-time UV monitoring, with accurate data successfully received by the host computer, validating the system's reliability and precision. This real-time monitoring system can not only reduce the manpower and material resources required for UV data collection, but also has a certain degree of significance for maintaining public health and environmental stability.

Keywords: Networking technology; ZigBee network; GPRS module, Remote transmission

1. INTRODUCTION

The Internet of Things technology (IoT), as an emerging technology, has been significantly promoted and transformed in various domains, with the development of the internet, the widespread application of sensors, and the increasingly sophisticated mobile technologies. The International Telecommunication Union proposed the Internet of Things in its 2005 annual report on the development of the world Internet. The report introduces the definition of the Internet of Things in detail and gives the research and development strategies of the Internet of Things cases in the United States and other countries.

IoT technological surge has notably revolutionized environmental monitoring, particularly in applications such as air quality assessment and climate observation. This technology enables real-time data acquisition through distributed sensor networks. Among the critical environmental factors, ultraviolet (UV) radiation stands out due to its profound implications for human health and ecological systems. Ultraviolet poses significant risks to human health, with long-term effects being particularly concerning for children and adolescents. Some studies [1-2] indicate that UV exposure leads to skin damage, and excessive exposure can lead to photoaging, an increased number of melanocytic nevi, and a higher risk of melanoma, especially in individuals with fair skin. UV is a major cause of basal cell carcinoma, squamous cell carcinoma, and cutaneous malignant melanoma, with artificial UV sources further elevating cancer risk [3]. Beyond skin damage, UV also harms ocular tissues, contributing to corneal pathologies, cataracts, glaucoma, and age-related macular degeneration. Children are particularly vulnerable due to their larger pupils and more transparent ocular media, with up to 80% of lifetime UV exposure occurring before age 18 [4]. In terms of ecology, Caldwell et al. [5] believed that UV radiation effects on plants, pathogens, herbivores, soil microbes and ecosystem processes below the surface. Meanwhile, UV's antimicrobial properties have been explored for public health applications, with far-UV (200–230 nm) showing potential in pathogen inactivation without harming human cells [6]. Consequently, the demand for real-time, efficient UV monitoring has intensified to safeguard public health and environmental stability.

Historically, UV monitoring has relied on costly meteorological stations, which, despite offering precise measurements, suffer from limited spatial coverage, high deployment and maintenance costs, and delayed data updates. These shortcomings render traditional methods inadequate for addressing the dynamic and spatially variable nature of UV radiation in modern environmental contexts.

In response, IoT technology emerges as a promising solution, realizing its capacity for low-cost, scalable, and real-time monitoring through interconnected sensor networks. For example, in recent years, the integration of IoT and wireless sensor networks (WSN) has opened new avenues for UV monitoring. ZigBee, a low-power WSN protocol, it is particularly popular in smart home devices, industrial automation, and healthcare due to its efficiency in short-range communication and minimal energy consumption [7-8]. To enhance its energy efficiency, innovations such as Passive-ZigBee have been introduced, which significantly reduce power consumption by converting WiFi signals into ZigBee packets, allowing heterogeneous IoT networks to interconnect [9]. Additionally, Zigbee plays a crucial role in wireless sensor networks (WSNs) and IoT-based automation, particularly in energy-efficient applications like smart lighting control [10]. For example, Liu et al. [11] established a system for short-range data acquisition.

The system sets up wireless sensor LAN network with ZigBee technology, and collects temperature and humidity and light intensity data to the coordinator node. Similarly, in the field of agriculture, Zhu et al. [12] used ZigBee nodes to monitor parameters such as temperature, humidity, and light in the Botanical Garden of Qiongzhou University. The research results show that these nodes can collect data in real time and transmit it to remote monitoring centers, demonstrating the practical application value of ZigBee in agricultural IoT. Frehill et al. [13] studied how to use ZigBee to connect vital sign monitors, ventilation fans, infusion pumps, and other devices to achieve centralized data collection. This study emphasizes the applicability of ZigBee in hospital environments, particularly in mobile patient monitoring.

Despite the advantages of ZigBee in real-time data acquisition for IoT applications, its communication range is limited to approximately 100 meters, restricting its deployment in large-scale or wide-area monitoring scenarios. This limitation highlights the need for a complementary technology to enable long-distance data transmission. To address this challenge, General Packet Radio Service (GPRS) has emerged as a robust solution for long-distance data transmission in remote monitoring systems. And it has been widely used in information transmission for ecological [14] and home environments [15]. For instance, Huang et al. [16], based on the GPRS technology, achieved the wireless real-time transmission of the remote monitoring data. And Liu et al. [11] used ZigBee networks to efficiently gather temperature, humidity, and light intensity data, relaying it to a coordinator node, which then transmits it to the internet via GPRS for remote access. Likewise, Wang et al. [17] presented a practical application of wireless networks: an online water monitoring system based on ZigBee and GPRS. Then the sensor data are collected and transmitted via ZigBee and GPRS.

However, the ZigBee+GPRS scheme's built-in routing algorithm may experience long transmission times in large-scale usage scenarios, due to the large number of network nodes. To solve this problem, Said [18] proposed a routing algorithm to optimize the selection of the best path for the transmitted data within the Internet of Things system. And he applies the most suitable ant colony algorithm to the concerned network within each area. But the improvement effect is still not significant.

The above examples highlight the complementary strengths of ZigBee and GPRS: ZigBee excels in local, energy-efficient data collection, while GPRS ensures reliable long-range transmission. However, existing studies predominantly focus on temperature or water quality, with comprehensive systems tailored to UV radiation monitoring receiving less attention. Although ZigBee and GPRS have made strides in environmental monitoring, their combined application to UV radiation remains underexplored. Therefore, for the above issues, this article proposes a remote real-time monitoring transmission system for ultraviolet data through combining ZigBee and GPRS technology. This system uses ultraviolet sensors to receive ultraviolet data, and then transmits the data to the Zigbee coordinator through the Zigbee self-organizing network. The GPRS module (includes SIM800 module) then transmitted data to the upper computer, where the dynamics of ultraviolet radiation can be monitored at all times, which is helpful for the research institute to analyze the data. At the same time, this article also introduced an ant colony particle + swarm routing optimization algorithm, which can find more suitable transmission paths in large-scale network environments and significantly reduce transmission latency. This real -time monitoring system can not only reduce the manpower and material resources required for UV data collection, but also is of great significance for maintaining public health and environmental stability.

2. Materials and Methods

As indicated in Table 1, the hardware material information necessary for establishing the real-time remote ultraviolet monitoring system in this study is provided.

Table 1. Hardware material information

The name of hardware	The role of hardware
UVM-30A sensor	measure ultraviolet data
CC2530 ZigBee module	as a coordinator or a router
Classic series SIM800 GPRS module	transmit the data to host computer
Host computer (PC)	display and store the collected data

This study leverages a self-constructed ZigBee network, integrated with a GPRS module, to achieve remote real-time monitoring of ultraviolet (UV) radiation. Additionally, based on existing routing rules, this study optimizes the routing protocols within the ZigBee network (ant colony and particle swarm optimization), thereby enhancing the data transmission speed. The specific process is outlined as follows:

The UVM-30A sensor periodically collects ultraviolet intensity data (e.g., UV index) from the environment.

The terminal device transmits the UV data to a nearby router or directly to the coordinator via the ZigBee protocol (IEEE 802.15.4, 2.4 GHz).

Optimize the routing algorithm of ZigBee network. After that, the coordinator receives UV data from terminal devices or routers, aggregating the data within the local network.

The coordinator forwards the UV data to the GPRS module, which encapsulates the data and transmits them to the public network. Simultaneously, the Peanut Shell service periodically updates the IP address, mapping the dynamic IP assigned by the GPRS network to a fixed domain name, ensuring stable access by the host computer.

The host computer operates the DTU toolbox software, accessing the GPRS via the Peanut Shell domain name. It receives TCP packets, parses the UV data for display, and stores the data using MySQL.

GPRS (General Packet Radio Service) is a new type of fast connection to the public network, based on the packet exchange protocol defined by the GSM standard. It can achieve uninterrupted connection between mobile terminals and networks, and adjust its network capacity according to data transmission, which can reduce network traffic con-sumption and lower usage costs.

Technical characteristics of GPRS:

The data transmission rate of GPRS is considerably high, reaching up to 170 kb/s. This advancement has replaced the reliance on dedicated dial-up Internet service providers for Internet access.

The high network throughput facilitates real-time online applications such as voice and video communication. Additionally, GPRS supports mobile packet-switched protocols, including the IP protocol and the X.25 protocol, enabling seamless Internet connectivity while enhancing the integrity and accuracy of data transmission. It also complements the short message service (SMS) and circuit-switched data service (CSD) of GSM. Furthermore, GPRS dynamically allocates bandwidth based on user requirements, optimizing the utilization of limited network resources. The shift from time-based to data-based billing has also contributed to cost reductions for users [19].

GPRS introduces additional hardware components into the GSM network, accompanied by corresponding software upgrades. The three key network hardware components introduced are the Serving GPRS Support Node (SGSN), the Gateway GPRS Support Node (GGSN), and the Packet Control Unit (PCU). The SGSN facilitates interactive operations between GPRS networks and external packet data networks. The packet-switching structure of GPRS enhances data transmission rates, reduces network resource consumption, and mitigates dial-up connection delays, thereby achieving seamless network connectivity.

1) GPRS Network Interface and Protocol:

GPRS adds new hardware devices on the basis of GSM, among which one type of SGSN is mainly used to record the location of mobile stations and complete the transmission and reception of mobile packet data between GGSNs and mobile stations [20]. The main function of GGSNs is to serve as gateways with routing capabilities, helping GPRS to better select transmission paths, achieve protocol conversion of data packets, and remotely transmit them to monitoring platforms.

As the air interface of GSM, Um's communication protocol consists of five layers from bottom to top: physical layer, medium access control layer (MAC), logical link control lay-er (LLC), subnet related aggregation protocol layer, and network layer [21]. The physical layer of the Um interface is the RF interface part, which provides various logical channels for Um. The carrier bandwidth of Um is 200kHz, with 8 physical channels available for use. Under ideal conditions, when all channels are active, the data transmission rate can reach 200 kb/s. This is an ideal state that can meet the requirements of data transmission and has certain practicality.

2) Data Transmission over GPRS Network:

The GPRS network is used for addressing and establishing data transmission routes. As for the external network, the GGSNs act as routers, implementing routing and ad-dressing functions between the GPRS backbone network and the external data network [22]. The establishment of data transmission routes includes setting up routes for sending data from a mobile station (MS), receiving data at an MS, and maintaining routes for an MS in a roaming state, thereby enabling seamless GPRS data transmission.

When a mobile station has a packet data unit, which sequentially passes through the fifth layer of the Um interface communication protocol to reach the users of the public data network, the data in the air interface Um can be encrypted and compressed using more secure DES or AES algorithms to ensure the security and efficiency of data transmission. For data reception, it is necessary to establish a connection gateway GPRS support node route according to the standard protocol of the public data network. The data unit is transmitted to the gateway GPRS support node through the established route, and then transmitted to the GPRS support node where the MS is located. The data is further encap-sulated into SNDC data units, processed by the LLC layer into LLC unit frames, and fi-nally transmitted to the MS over the air interface Um.

When transmitting data to a roaming user, the data must first pass through the GPRS support node at the home location before reaching the user, and then be sent and received through routing addressing.

ZigBee networks consist of three types of nodes: coordinators, routers, and terminal devices. The primary function of a coordinator is to establish the network and manage the joining and departure of other devices. Routers participate in the network as intermediary nodes, facilitating communication between terminal devices and the coordinator while also optimizing routing paths. Terminal devices can join the network to send and receive data but lack the capability to relay messages. Both ZigBee coordinators and routers are classified as Full-Function Devices (FFDs).

1) Three topologies of ZigBee:

ZigBee networks support three types of topologies: star topology, tree topology, and mesh topology. The structures of these topologies are illustrated in Figure 1. The star topology follows a point-to-multipoint communication protocol; the tree topology establishes routing paths based on hierarchical levels; and the mesh topology integrates Z-AODV with hierarchical tree routing.

Each ZigBee topology has distinct characteristics. The star topology consists of a central coordinator (ZC) and multiple end devices (ZEDs). The coordinator is responsible for network formation and maintenance, while end devices operate within the coordinator's communication range. These terminal nodes are independent of each other and can only transmit data to the coordinator. As the star topology does not require network-layer protocols, it represents a simple structure suitable for networks with a limited number of nodes.

The tree topology comprises a coordinator, multiple routers, and terminal nodes. Router nodes typically function as leaf nodes, and each node can only communicate directly with its parent or child nodes. Although the tree topology covers a large area, its reliance on a single transmission path leads to potential delays and limited redundancy, which are significant drawbacks. The mesh topology is an enhanced version of the tree topology, extending its single-path routing mechanism by allowing routers to maintain routing tables and establish multiple paths for data transmission. Unlike the tree topology, mesh topology enables peer-to-peer communication between network nodes and includes multiple coordinators and routers. Each node can communicate within its coverage area, but a designated coordinator is still required to aggregate information. Mesh networks exhibit high reliability and self-recovery capabilities; if one path becomes obstructed, alternative routes ensure uninterrupted data transmission. By enabling multiple simultaneous transmission paths, the mesh topology improves data transmission efficiency. However, it also increases data volume and imposes higher storage requirements [23].

Figure 1. Topological Structure Functions of Routing

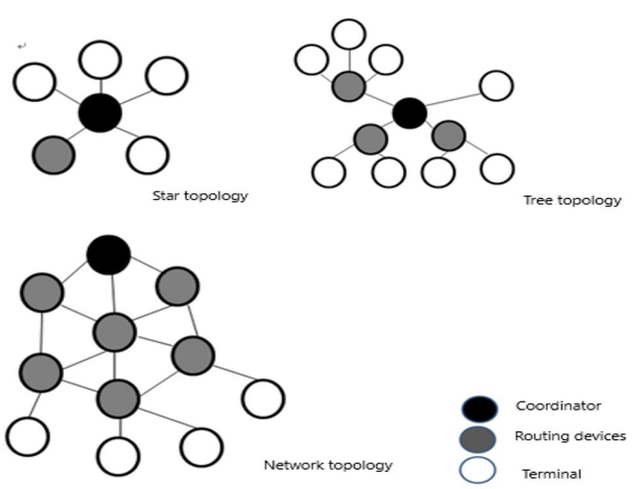

2) Routing technology of ZigBee:

In ZigBee networks, the Ad-hoc On-demand Distance Vector (AODV) routing protocol or its simplified version, AODVjr, is commonly used to implement routing functions. The AODV protocol discovers paths by broadcasting route request (RREQ) messages on demand. When a node receives the first route request, it replies with a route response (RREP) to establish the shortest path. However, this protocol has high routing overhead and energy consumption, reducing efficiency in large-scale networks. The tree routing algorithm defined in the ZigBee specification utilizes a Distributed Address Assignment Mechanism (DAAM) to establish fixed paths, thereby lowering routing maintenance costs. However, it suffers from problems such as path detours and traffic concentration, which can degrade network performance.

The AODVjr routing protocol is a simplified version of the AODV algorithm, omitting complex mechanisms such as sequence numbers, Hello messages, and route error (RERR) notifications. This makes it more suitable for resource-constrained ZigBee networks. Its route discovery process is relatively simple, relying solely on route request (RREQ) and route response (RREP) messages for path selection and establishment. The core mechanism of AODVjr route discovery is as follows: When a source node S needs to send data to an unknown destination node D, it broadcasts a route request (RREQ). Intermediate nodes forward the first received request, and once the destination node receives the RREQ, it replies with a route response (RREP). This response propagates back to the source node hop by hop along the established path, forming a unique and fixed routing path.

The Particle Swarm Optimization (PSO) algorithm is a swarm intelligence optimization algorithm that mimics the collective behavior of bird flocks or fish schools. It searches for the optimal solution based on the global information of the entire particle swarm. The PSO algorithm achieves optimization by updating each particle's position and velocity, with its core update equations given as follows:

$$v_i^{k+1} = wv_i^k + c_1 r_1 (p_{best} - x_i) + c_2 r_2 (g_{best} - x_i)$$

Among them, v is the particle velocity; x is the position; Pbest is the historical optimal position of the particle; gbest is the historical best position of the group; C1 and C2 are learning factors; ω is the inertia weight.

The Ant Colony Optimization (ACO) algorithm solves optimization problems by simulating the cooperative mechanism of ants searching for food paths. It updates path selection probabilities using pheromone trails, with its core probability update equation given as follows:

$$P_{ij}^k(t) = rac[au_{ij}(t)]^\alpha [\eta_{ij}]^e ta \sum_{u \in allowed} [au_{iu}]^\alpha [\eta_{iu}]^e ta$$

Among them, au_{ij} represents the pheromone concentration of path (i, j), η_{ij} is the heuristic information of path (i, j) (usually the reciprocal of path length), and α represent the importance of pheromone information.

The PSO+ACO hybrid algorithm integrates the advantages of both PSO and ACO. It leverages PSO's capability for rapid global search and ACO's ability for precise path optimization, significantly improving the overall performance of routing algorithms. In large-scale node networks, the PSO-ACO algorithm effectively reduces path redundancy and network latency while maintaining reasonable energy consumption, thereby enhancing overall network performance.

3. Results and Discussion

A. Routing Algorithm Optimization Experiment

Although the Cluster Tree topology is widely used in practical applications due to its clear parent-child relationship and ease of maintenance, this study focuses on its generality and conducts routing algorithm optimization experiments on both Cluster Tree and Mesh topologies. By comparing the path discovery time and transmission time under different node numbers, the optimization effect of ACO+PSO routing algorithm compared to AODVjr routing algorithm is verified. The optimization objective of this article is limited to path efficiency, assuming that the address allocation for each node has been completed.

This experiment used the NetworkX library to simulate the ZIgBee topology structure and built it in two commonly used ZigBee topologies (tree topology Tree and mesh topology Mesh). The node connection settings for the two topology structures are as follows:

1) As shown in Figure 2 (a), in the Mesh network topology, we adopt the following connection rules: the coordinator node is located at the center of the network, the router node can be connected to any other router or coordinator node within the communication radius, and the end device can only be connected to the coordinator or router node within its communication radius. The connection radius between nodes is set to 50 meters, which means that only nodes with a distance less than 50 meters can establish direct connections. To simulate the actual network environment, we have limited the connection capabilities: routers can connect up to 15 nodes, and coordinators can connect up to 30 nodes.
2) As shown in Figure 2 (b), in the Tree network topology, we adopt the following connection rules: the coordinator node serves as the root node (the first layer of the tree), the router node serves as the intermediate node, distributed from the second to the fourth layer, and the terminal node serves as the leaf node, located at the bottom layer (mainly the fifth layer). Each parent node can connect up to 3 child nodes, and the path strictly follows the parent-child hierarchical relationship, without allowing cross layer connections.

Figure 2. Network topology

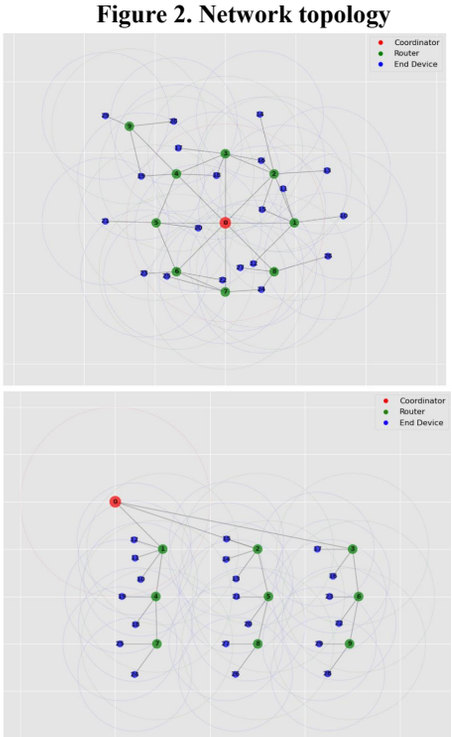

(a) Mesh topology (b) Tree topology

AODVjr, as a commonly used lightweight routing protocol in ZigBee networks, implements a simplified version of the AODV protocol, removing many complex functions such as link state monitoring and preventive routing maintenance to adapt to the resource limitations of ZigBee devices.

In our implementation, each node maintains a simple routing table that records information such as destination address, next hop address, hop count, and sequence number. We have configured it as follows: it uses on-demand broadcasting for route discovery, with the minimum hop count as the main selection criterion. When a node receives routing information, if the sequence number of the new information is greater than the original record, it unconditionally updates the routing table; If the serial number is the same but the number of hops is less, an update will also be triggered. The protocol sets a 60 second routing timeout mechanism, after which the corresponding routing entry automatically becomes invalid. Meanwhile, to control network overhead, the maximum hop count is limited to 10 hops, and routing requests exceeding this limit will be ignored.

We introduce a hybrid algorithm ACO+PSO that combines ant colony optimization (ACO) and particle swarm optimization (PSO) to improve the routing efficiency of ZigBee networks. Among them, the commonly used parameters in the ACO algorithm include setting the initial pheromone value to 1.0, ensuring that all path edges have the same initial value, increasing the pheromone intensity Q by 100, and the pheromone update mechanism depends on the path length. During network operation, the increase in pheromone intensity and update mechanism are influenced by the pheromone volatilization factor ρ=0.1 for updates. The number of ants is dynamically adjusted according to the network size, with a range controlled between 10 and 30 individuals.

In terms of PSO algorithm, the inertia weight of particles dynamically changes during the algorithm iteration process to balance global and local search capabilities, with a set range between 0.6 and 0.9, and the specific value is dynamically adjusted according to the node size. In terms of learning factors, both individual learning factor (c_1) and social learning factor (c_2) are fixed at 2.0. The number of particles is dynamically adjusted between 20 and 40 based on the size of the network, and the maximum number of iterations for the algorithm is between 50 and 90 to ensure effective convergence at an acceptable computational cost. The specific parameters are shown in Table 2.

Table 2. Hardware material information

Algorithm	Parameter	value
ACO	initial pheromone value	1.0
	pheromone intensity Q	100
	pheromone volatilization factor ρ	0.1
	number of ants	10-30
PSO	inertia weight ω	0.6-0.9
	individual learning factor c1	2.0
	individual learning factor c2	2.0
	number of particles	20-40
	maximum number of iterations	50-90

We introduce the collaborative working mechanism of ACO+PSO algorithm as follows: The algorithm process first initializes the network parameters, including setting the initial pheromone values of all network paths to a uniform value of 1.0, and dynamically determining the number of ants, particles, and iterations. Next, in the ACO path construction phase, each ant starts from the source node and selects the next hop node based on the concentration of pheromones and heuristic information (including inter node distance, node type, and link quality) along the path, until reaching the destination node. Subsequently, ants record path information and update pheromone distributions to provide initial solutions for the PSO algorithm.

In the PSO optimization stage, we convert the paths generated in the ACO stage into the initial positions of particles in the particle swarm algorithm, with each particle corresponding to a possible routing path. During the PSO iteration process, particles update their speed and position based on their current position, individual historical best position (p_best), and population historical best position (g_best). The core update formula is:

$$V(i+1) = \omega \times V(i) + c_1 \times rand() \times (p_{best} - X(i)) + c_2 \times rand() \times (g_{best} - X(i))$$

Among them, the inertia weight ω is dynamically adjusted between 0.6 and 0.9 to balance global and local search; The individual learning factor c1 and the social learning factor c2 are both set to 2.0. The path quality is determined by the comprehensive energy consumption, transmission delay, and hop count. After each iteration, update the pheromone concentration of the path using the following formula:

$$\tau(i,j) = (1-\rho)\tau(i,j) + \Delta\tau(i,j)$$

The increase in pheromone content $\Delta\tau(i,j)$ is directly proportional to the path quality, and the pheromone volatilization rate ρ set to 0.1.

In addition, we dynamically adjust the number of ants (10 to 30), the number of particles (20 to 40), and the maximum number of iterations of the algorithm (50 to 90) based on the network size, and set the termination condition of the algorithm to reach the maximum number of iterations or achieve a path quality improvement of less than 1% for multiple consecutive iterations. This optimization process ensures that the algorithm runs efficiently in resource constrained ZigBee networks and can effectively improve routing efficiency and network performance.

The main evaluation metrics of this experiment are the path discovery time and transmission time. Path discovery time refers to the time required from initiating a routing request to obtaining a complete routing path, reflecting the real-time performance of the algorithm. The transmission time is defined as the total time required for a data packet to be transmitted from the source node to the destination node. The specific calculation method is the sum of the transmission times of each link on the path, that is, the transmission time is equal to the sum of the individual transmission times of all links. The formula for calculating the transmission time t is:

$$t(i,j) = t_{base} \times (1 + F_{dist}) \times (1 + F_{type}) \times (1 + F_{cong})$$

Among them, the basic transmission time tbase is set to 0.01 seconds, determined based on the ZigBee standard data transmission rate and standard packet size; The distance factor Fdist is the ratio of the actual distance d(i, j) between nodes to the maximum communication distance dmax; The value of the node type factor Ftype is determined based on the node type, with 0.1 for coordinators, 0.3 for routers, and 0.5 for terminal nodes; The congestion factor Fcong is defined as the ratio of the current number of connections of node i to the maximum number of connections of node i.

We applied two algorithms to the commonly used mesh and tree network structures in ZigBee for experimentation. In the experiment, due to the relatively simple network structure of the tree, the number of nodes in this topology gradually increased from 10 to 200, while in the mesh network structure, the number of nodes was expanded from 10 to 500. Each configuration was tested 5 times and the average was taken. The communication path from the farthest terminal node to the coordinator node was selected for comparative analysis.

As shown in Figure 3, in the mesh topology structure, in order to simulate the real situation, we randomly increase the positions of terminals and routing nodes, and increase the number of network nodes from 10 to 500. The experimental results show that as the network size expands, the performance gap between ACO+PSO algorithm and AODVjr algorithm gradually widens, and the transmission time of AODVjr algorithm rapidly increases from 0.16 seconds to 0.80 seconds. The transmission time of the ACO+PSO algorithm shows a more gradual logarithmic growth, increasing from 0.17 seconds to 0.48 seconds, an increase of 1.8 times. Especially when the number of nodes reaches 500, the transmission time of ACO+PSO algorithm is reduced by about 40% compared to AODVjr algorithm. The main reason for ACO+PSO's excellent performance in mesh topology is that it can effectively utilize the multiple alternative paths provided by the mesh topology structure, and successfully avoid high load areas by intelligently analyzing node types, load conditions, and congestion levels. Meanwhile, with the expansion of network scale, although there are more available paths, the complexity also increases. However, the ACO+PSO algorithm, through its adaptive learning mechanism, can find approximate optimal solutions in complex environments and maintain a low transmission delay growth rate.

Figure 3. Transmission time comparison in mesh topology

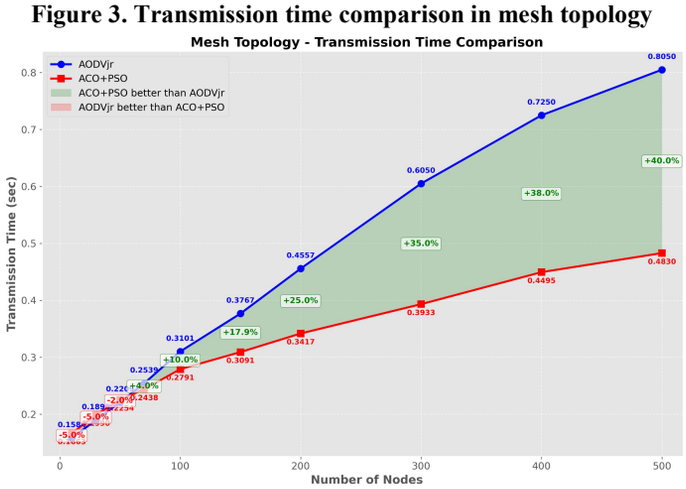

As shown in Figure 4, in the tree topology, we conducted experiments by gradually increasing the number of terminal and router nodes (from 10 to 200), and the results obtained were consistent with theoretical expectations. Experimental data shows that due to the strict hierarchical structure of the tree topology itself, which significantly limits the flexibility of path selection, the ACO+PSO algorithm did not demonstrate significant performance advantages over the AODVjr algorithm in this scenario. For example, when the number of nodes is 30, the transmission time of ACO+PSO algorithm is about 13.5% higher than AODVjr. When the node size increases to 200, the average transmission time of ACO+PSO is about 21.5% higher than AODVjr. This result indicates that the limitations of path selection in tree topology constrain the optimization potential of ACO+PSO algorithm based on swarm intelligence. In addition, the computational complexity of ACO+PSO algorithm is higher, and the additional computation time required for path discovery process also increases, resulting in a decrease in its transmission efficiency in such topology structures.

Figure 4. Transmission time comparison in tree topology

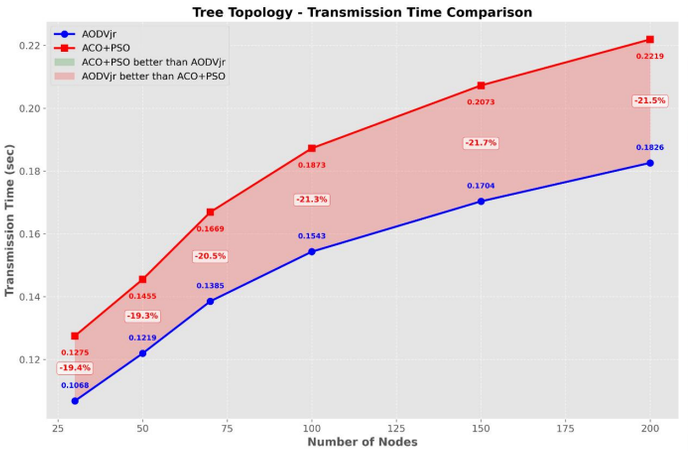

As shown in Figure 5, experimental analysis shows that the ACO+PSO algorithm has significant differences in path discovery time compared to the AODVjr protocol. In all topology structures, the path discovery time of ACO+PSO algorithm is significantly longer than AODVjr. This phenomenon is consistent with theoretical expectations, as ACO+PSO, as an optimization algorithm based on swarm intelligence, requires multiple rounds of iterative calculations and information exchange to obtain the optimization path. Specifically, as the number of nodes increases, the path discovery time of ACO+PSO increases more significantly. For example, in mesh topology, as the number of nodes increases from 50 to 500, the path discovery time of ACO+PSO increases from about 0.27 seconds to over 30 seconds, while AODVjr increases from 0.00005 seconds to 0.0008 seconds, with almost no change. This indicates that in scenarios with extremely high real-time requirements, it is necessary to balance the comprehensive impact of path discovery time and transmission time.

Figure 5. Path discovery time comparison in two topologies

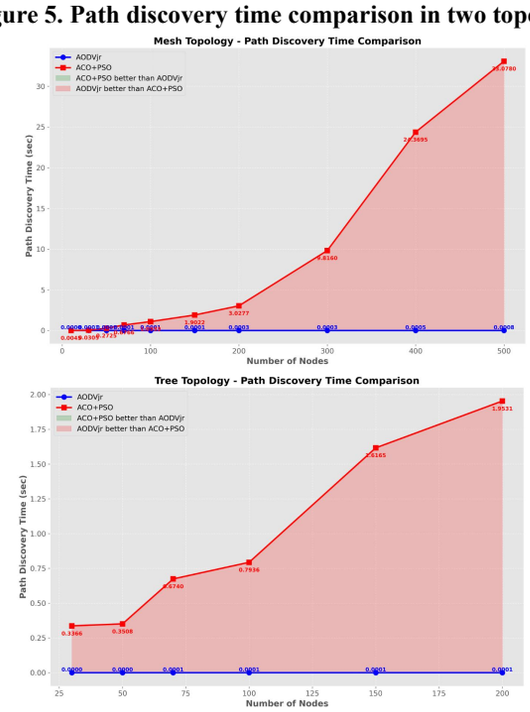

(a) Mesh topology (b) Tree topology

Based on experimental data, a comprehensive performance analysis was conducted on the Tree and Mesh topologies. The results showed that in the Tree topology, due to limitations in path selection, the ACO+PSO algorithm had an overall transmission time that was about 20% higher than the AODVjr algorithm. This suggests that in a strictly hierarchical network, the simple and efficient AODVjr may be more suitable. The ACO+PSO algorithm has the most significant advantage in the mesh topology structure. As the number of nodes increases from 50 to 500, its performance advantage expands from a slight difference in the initial stage to about 40% in the later stage. The

ACO+PSO algorithm exhibits excellent scalability in large-scale mesh topologies, with a significantly smoother transmission time growth curve than AODVjr, and can maintain relatively stable transmission performance in complex network environments. In summary, although the ACO+PSO hybrid algorithm has the problem of long path discovery time, its transmission time advantage in large-scale complex networks is very significant. Especially in mesh topologies with over 100 nodes, the ACO+PSO algorithm can maintain a low transmission delay growth rate, making it more suitable for frequent data transmission and high load application scenarios; In tree topology or small-scale simple networks, considering comprehensive performance factors, AODVjr may be a more cost-effective choice. This result has important guiding significance for the practical application of ZigBee networks.

B. ZigBee performance testing

In the testing of ZigBee networking performance, a fixed coordinator node, two router nodes, and two UV sensor terminal nodes were selected for the networking test. First, the entire testing system is powered on, a network is established with the coordinator, and fixed network addresses are assigned to the two router nodes. The router nodes are part of the network, and the ultraviolet sensor terminal nodes must seek to join the network by issuing requests, communicating with the router nodes. LED indicator lights are used to show that the terminal nodes are operational. If the movement of UV sensor terminal nodes exceeds the effective range, the terminal nodes will disconnect from the network. When they return within the effective distance, they will reconnect to the network. This demonstrates that ZigBee has self-organizing capabilities, making the network stable and reliable.

In the laboratory environment, a fixed ZigBee coordinator node is chosen to directly connect to the upper computer, while a terminal node is selected for ultraviolet sensor data collection to test the distance performance with the fixed ZigBee coordinator. First, the testing system is powered on, and then the upper computer sends a command to collect ultraviolet data. The coordinator forwards the command to the ultraviolet terminal node, and the ultraviolet sensor on the terminal node begins to collect ultraviolet radiation data. The collected data is transmitted to the monitoring platform of the upper computer through the coordinator. We gradually increase the distance between the ultraviolet sensor terminal node and the coordinator node, using the packet loss rate to determine performance standards. A 2.4 GHz transmission frequency is selected for testing, with a power of 0 dBm and a packet loss rate of no more than 5% to meet the standard. During the testing process, interference from other factors is eliminated. The relationship between short-range communication and packet loss rate is shown in Table 3.

Table 3. Relationship between Short Distance Communication and Packet Loss Rate

Distance/m	Sent data packet(pc)	Received data packets(pc)	Packetloss rate (%)
10	200	200	0
20	200	200	0
30	200	200	0
40	200	200	0
50	200	200	0
60	200	200	0
70	200	198	1
80	200	190	5
90	200	182	9
100	200	168	16

From Table 3, it can be concluded that packet loss occurs at a distance of 70m from the UV sensor terminal node to the coordinator node. Within a radius of 80m, the packet loss rate that meets the requirements shall not exceed 5%. After 90m, the packet loss rate and express delivery increase. Through testing, it can be concluded that ZigBee is a short-range wireless transmission communication technology that requires ensuring data transmission within an effective distance to ensure the integrity and accuracy of data transmission.

In addition, this section also tested the relationship between packet transmission frequency and packet loss when the communication distance is constant. The result is shown in Table 4.

Table 4. Relationship between Interval of per data packet and Packet Loss Rate

Interval/s	Sent data packet(pc)	Received data packets(pc)	Packet loss rate (%)
10	200	200	0
5	200	199	0.5
2	200	198	1
1	200	195	2.5
0.5	200	190	5
0.2	200	180	10
0.1	200	160	20
0.05	200	140	30

Given a constant communication distance, an increased interval between sending data packets leads to a decreased packet loss rate, whereas a decreased interval leads to an increased rate. Because when the packet transmission time is too short, it will cause data to converge to the coordinator node, resulting in data congestion and packet loss. Therefore, in addition to being within an effective distance range, it is also necessary to ensure a suitable packet transmission time interval, which can better transmit data, make the data more complete to be received in the upper computer monitoring center, and reduce packet loss rate in the process of ultraviolet data collection.

C. System acquisition function testing

After setting up the preceding ZigBee network, the next step is to determine whether the GPRS module and the upper computer are functioning properly by checking if the upper computer can receive ultraviolet data correctly.

The ultraviolet sensor selects the optimal routing path through ZigBee technology's self-organizing network, collects data, and transmits it to the GPRS module. By mapping the internal network address and port of the Peanut Shell, remote transmission of the collected information is achieved via a mobile phone card. The main computer receives the transmitted data through the DTU toolbox. The DTU toolbox receives an output voltage ranging from 0 to 1V, corresponding to a UV index from 0 to 10. The output voltage is converted into a UV index, and the collected data is stored in the upper computer's MySQL database and displayed in real-time in the LabVIEW environment.

In the test, the ZigBee network consists of a coordinator node, a router node, and a ZigBee ultraviolet collection terminal node. By analyzing the ultraviolet monitoring data collected by the upper computer, real-time monitoring of ultraviolet radiation can be achieved, completing the collection and remote transmission of ultraviolet radiation, and storing and displaying the data in real-time in the upper computer's monitoring center.

It has been successfully demonstrated that the system constructed in this paper can achieve real-time remote monitoring of ultraviolet radiation, by comparing the collected ultraviolet radiation under three conditions of sunny, cloudy, and rainy days with the ultraviolet index of the meteorological station. The specific UV collection data is shown in the table below (Table 5,6,7).

Table 5. Comparison between UV Collection Index and Meteorological Observatory Index during Sunny Days

Time (sunny)	Collection index (UV)	Meteorological Observatory Index (UV)
07:00	5	5
08:00	5	5
09:00	6	6
10:00	8	8
11:00	10	10
12:00	10	10
13:00	10+	12
14:00	10+	12
15:00	10+	12
16:00	10+	12
17:00	10	12
18:00	10	11
19:00	6	6
20:00	3	3

Table 6. Comparison between UV Collection Index and Meteorological Observatory Index during Cloudy Days

Time (cloudy)	Collection index (UV)	Meteorological Observatory Index (UV)
07:00	2	2
08:00	3	3
10:00	8	8
11:00	8	8
12:00	8	8
13:00	9	9
14:00	9	8
15:00	9	9
16:00	10	9
17:00	10	11
18:00	9	9
19:00	5	5
20:00	2	2

Table 7. Comparison between UV Collection Index and Meteorological Observatory Index during Rainy Days

Time (rainy day)	Collection index (UV)	Meteorological Observatory Index (UV)
07:00	2	2
08:00	2	2
09:00	3	3
10:00	4	4
11:00	6	7
12:00	7	8
13:00	7	7
14:00	8	8
15:00	8	6
16:00	8	9
17:00	7	9
18:00	5	5
19:00	3	3
20:00	1	1

4. Conclusions

ZigBee networking technology and GPRS technology have achieved short distance and remote transmission of ultraviolet wireless sensor networks. After comparison, UVM-30A is selected as the ultraviolet sensor, CC2530 core board is selected as the ZigBee module, and the classic series SIM800 module is selected as the GPRS module, which re-alizes the collection and transmission of ultraviolet data.This design has completed the following aspects of work:

We conducted routing algorithm optimization experiments on both Cluster tree and Mesh topologies. In tree topology or small-scale simple networks, considering comprehensive performance factors, AODVjr may be a more cost-effective choice. In mesh topologies with multiple nodes, the ACO+PSO algorithm can maintain a low transmission delay growth rate, providing an effective solution for the IoT scenario of large-scale network node data transmission.

The characteristics of ZigBee self-organizing network have been verified. And through testing, it can be concluded that ZigBee is a short-range wireless transmission communication technology that requires ensuring data transmission within an effective distance to ensure the integrity and accuracy of data transmission. Given a constant communication distance, an increased interval between sending data packets leads to a decreased packet loss rate, whereas a decreased interval leads to an increased rate.

Finally, the GPRS module and upper computer were verified by checking if the upper computer can receive ultraviolet data correctly. It has been successfully demonstrated that the system constructed in this paper can achieve real-time remote monitoring of ultraviolet radiation.

On the basis of existing design and research, there are many aspects of this study that can be optimized and expanded. In the field of routing algorithms in ZigBee technology, although current research has achieved certain results, there is still potential for improvement. The existing routing algorithms still need to improve their efficiency when dealing with complex network environments. In the future, more advanced algorithm models can be further studied, combined with artificial intelligence and machine learning technologies, to make routing optimization more intelligent and efficient. For example, deep learning algorithms can be used to predict and analyze the behavior and data traffic of network nodes, plan the optimal routing path in advance, and reduce data transmission latency. In addition, the computational complexity of the algorithm can be further optimized to reduce its consumption of system resources, enabling ZigBee networks to maintain efficient operation even under resource constraints. During remote data transmission, better data fusion can be achieved, reducing interference to data during transmission and improving the accuracy of remote data transmission. The upper computer platform can be more user-friendly, adding more functions according to needs.

REFERENCES

[1] Xiaoyou Tang, Tingyi Yang, Daojiang Yu, Hai Xiong, Shuyu Zhang. Current insights and future perspectives of ultraviolet radiation (UV) exposure: Friends and foes to the skin and beyond the skin [J]. Environment International, 2024, 185:108535

[2] Adèle C. Green, Wallingford S C , Mcbride P .Childhood exposure to ultraviolet radiation and harmful skin effects: Epidemiological evidence [J]. Progress in Biophysics and Molecular Biology, 2011, 107(3):349-355.DOI:10.1016/j.pbiomolbio.2011.08.010.

[3] Dermatology S O , Balk S J .Ultraviolet radiation: a hazard to children and adolescents.[J].Pediatrics, 2011, 127(3):588.DOI:10.1542/peds.2010-3501.

[4] Ivanov IV, Mappes T, Schaupp P, Lappe C, Wahl S. Ultraviolet radiation oxidative stress affects eye health [J]. Biophotonics. 2018; 11:e201700377. https://doi.org/10.1002/jbio.201700377.

[5] Caldwell MM, Bornman JF, Ballaré CL, Flint SD, Kulandaivelu G. Terrestrial ecosystems, increased solar ultraviolet radiation, and interactions with other climate change factors [J]. Photochem Photobiol Sci, 2007, 6(3): 252-66. DOI: 10.1039/b700019g.

[6] Hessling M, Haag R, Sieber N, Vatter P. The impact of far-UVC radiation (200-230 nm) on pathogens, cells, skin, and eyes - a collection and analysis of a hundred years of data [J]. GMS Hyg Infect Control. 2021 Feb 16;16:Doc07. doi: 10.3205/dgkh000378. PMID: 33643774; PMCID: PMC7894148.

[7] Zohourian A , Dadkhah S , Neto E P ,et al. IoT Zigbee device security: A comprehensive review [J]. Internet Things, 2023, 22:100791.DOI:10.1016/j.iot.2023.100791.

[8] W. Wang, G. He and J. Wan. Research on Zigbee wireless communication technology [C]. 2011 International Conference on Electrical and Control Engineering, Yichang, China, 2011, pp. 1245-1249, doi: 10.1109/ICECENG.2011.6057961.

[9] Li Y , Chi Z , Liu X ,et al.Passive-ZigBee: Enabling ZigBee Communication in IoT Networks with 1000X+ Less Power Consumption [J]. ACM, 2018.DOI:10.1145/3274783.3274846.

[10] Varghese S G , Kurian C P , George V I ,et al.Comparative study of zigBee topologies for IoT-based lighting automation [J]. Wireless Sensor Systems, IET, 2019.DOI:10.1049/iet-wss.2018.5065.

[11] L. Liu and W. Jiang. Design of vegetable greenhouse monitoring system based on ZigBee and GPRS [C]. 2018 4th International Conference on Control, Automation and Robotics (ICCAR), 2018, pp: 336-339. DOI: 10.1109/ICCAR.2018.8384696.

[12] Xiaojing ZHU, Yuanguai LIN. ZigBee Implementation in Intelligent Agriculture Based on Internet of Things [C]. Proceedings of the 2nd International Conference on Electronic & Mechanical Engineering and Information Technology (EMEIT 2012), 2012. DOI: 10.2991/emeit.2012.408.

[13] Frehill P, Chambers D, Rotariu C. Using Zigbee to integrate medical devices [C]. Annu Int Conf IEEE Eng Med Biol Soc, 2007:6718-21. DOI: 10.1109/IEMBS.2007.4353902.

[14] Deng Xiaolei, Li Minzan, Wu Jia, Che Yanshuang, Zheng Lihua. Development of mobile soil moisture monitoring system integrated with GPRS, GPS and ZigBee [J]. Transactions of the Chinese Society of Agricultural Engineering, 2012, 28: 130-135.

[15] Yang F, Liu C, Pei Z, et al. The design of wireless remote intelligent home system based on Zigbee and GPRS [C]. Iet International Conference on Communication Technology & Application.IET, 2012.DOI:10.1049/cp.2011.0756.

[16] M. Huang and Y. Wu. Environmental Monitoring System Based on GIS and Wireless Communications [C]. 2010 4th International Conference on Bioinformatics and Biomedical Engineering, 2010, pp:1-4. DOI: 10.1109/ICBBE.2010.5515959.

[17] Wang X, Ma L, Yang H. Online Water Monitoring System Based on ZigBee and GPRS [J]. Procedia Engineering, 2011, 15:2680-2684. DOI:10.1016/j.proeng.2011.08.504.

[18] Omar Said. Analysis, design and simulation of Internet of Things routing algorithm based on ant colony optimization [J]. International Journal of Communication systems, 2016, 30(8).

[19] Sooväli, L., Rõõm, E. I., Kütt, A., Kaljurand, I., & Leito, I. Uncertainty sources in UV-Vis spectrophotometric measurement. Accreditation and quality assurance, 11, 246-255.

[20] KonradKleszczyski, Stephanie Zwicker, Stefan Tukaj, Michael Kasperkiewicz, Detlef Zillikens, Ronald Wolf, Tobias W. Fischer.Melatonin compensates silencing of heat shock protein 70 and suppresses ultraviolet radiation-induced inflammation in human skin ex vivo and cultured keratinocytes.J. Pineal Res., 2015, Vol.58 (1).

[21] Maghsoodi Moghadam, R., Farasati, F., Toolabi, A., & Jafarzadeh, Z. (2014). Light intensity and ultraviolet radiation in the libraries and computer sites of Ilam Universities. Health and Development Journal, 2(4), 316-325.

[22] Bonabeau E, Dorigo M, Theraulaz G.Swarm intelligence:From natural to artificial systems[M]. New York:Oxford University Press, 1999:40-58.

Elizabeth K. Cahoon;; Ruth M. Pfeiffer;;David C. Wheeler;;Juan Arhancet;;Shih-Wen Lin;;Bruce H. Alexander;;Martha S. Linet;;D. Michal Freedman, Int. J. Cancer, 2015, Vol.136 (5)

.